Published in: International Journal of Mass Spectrometry and Ion Processes (1995), vol.. 148, pp. L17-L23.
Status: Postprint (Author's version)

The dissociative ionization of carbon dioxide below 21.22eV. A high resolution PIPECO spectroscopic investigation

R. Locht

Département de Chimie Générale et de Chimie Physique, Institut de Chimie, Bât. B6, Université de Liège, Sart-Tilman par B-4000 Liège 1, Belgium

Abstract

The photoion-photoelectron spectrum of O^+, CO^+ and CO_2^+ has been investigated under high resolution conditions. The O^+ ion production is found not to be restricted to the CO_2^+ ($C^2\Sigma_g^+$,0,0,0) predissociation. The (0,1,0) and (1,0,0) levels are clearly shown to be involved. The CO^+ ion production involves all the vibrational states reached in the Franck-Condon region, i.e. up to (2,0,1) at 19.94eV. Branching ratios were measured. The CO_2^+ molecular ion does not survive the predissociation in the entire energy range covered in the present work.

Keywords*:* Carbon dioxide; Coincidence; Dissociation; Kinetic energy; Photoionization

1. INTRODUCTION

The dissociative ionization of CO_2 in the valence-shell ionization region has been investigated by almost all the techniques available today. The literature on this subject has been reviewed recently [1]. By high resolution photoionization mass spectrometry and threshold photoelectron spectroscopy the major importance of autoionization in the appearance of O^+ and CO^+ has been demonstrated [2-5]. By photoelectron photoion coincidence (PIPECO) experiments, using the He(I) resonance line at 58.4nm, only the CO^+ and O^+ dissociation channels are accessible energetically [6,7]. To our knowledge, only one coincidence experiment has been performed on the dissociative ionization of CO_2 using synchrotron radiation [4]. In the latter case, the investigation was limited to the production of O^+ and CO_2^+only. The experiments covering the three dissociative ionization channels of CO_2 into CO^+, O^+ and C^+ mainly used the electroionization mass spectrometric technique [1]. The energies range from the onset up to l00eV impinging electron energy. Using synchrotron radiation, these three fragmentation channels were investigated by mass spectrometric photoionization between 35 and 60eV photon energy [8]. There are very few studies which include the translational energy measurements of the fragment ions [1].

Previously, we reported a detailed study of the dissociative electroionization of CO_2 in its three dissociation channels, covering the electron energy range from 19 to 40eV [1]. This investigation included the experimental determination of the translational energy of the fragment ions at threshold. The aim of the present work is to carry out the electron impact work by using our newly operating PIPECO experiment which allows us to obtain coincidence spectra without considerably altering the resolution of the photoelectron spectrometer. The latest work on O^+ and CO^+ formation from CO_2 is by Bombach et al. [7]. They measured coincidences and branching ratios for discrete values, i.e. for three vibrational levels of the CO_2^+ ($C^2\Sigma_g^+$) state, with a resolution of 75 meV under coincidence conditions. The aim of this Letter is to report on coincidence spectra recorded for CO^+, O^+ and CO_2^+ with 30meV resolution. Branching ratios for nearly all vibrational levels of the $C^2\Sigma_g^+$ state of CO_2^+ could be measured. Only the Fermi resonance doublet (1,0,0/0,2,0) [9] could not be resolved under these conditions.

2. EXPERIMENTAL

The experimental apparatus used in the present work will be described in detail elsewhere [10]. In this Letter, we limit the description to the most prominent features.

The gaseous sample is introduced into the ion chamber by an effusive gas inlet. The ion chamber is a cylindrical housing 9 mm in height and 20 mm in diameter covered on both sides by tungsten mesh of 70 lines per inch (LPI). This geometry is also used to ensure that the three perpendicular directions, i.e. the axis of the ion and electron optics, the light capillary and the light detection system and finally the gas inlet system when a hypodermic needle is used, intersect at the central point of the ionization region. The ion optics executed on the basis of ion optical calculations, is made of two triplet lenses located on either side of a focusing lens. Photoions,

extracted with a weak electric field (typically 100 mV cm^{-1}), are focused on the entrance hole of a quadrupole mass spectrometer (Balzers QMG 311). Coaxially, in the opposite direction to the ions, photoelectrons are extracted and analysed in a retarding potential based photoelectron spectrometer characterized by a differential output, designed and described by Lindau et al. [11]. This spectrometer is built of two sets of seven cylindrical lenses mounted symmetrically with respect to a central retarding grid (tungsten mesh of 70 LPI). A circular plate, spot-welded on this grid, prevents the light and straight-flying electrons from reaching the detector. Both the photoion source and the photoelectron spectrometer are surrounded by two concentric μ-metal cylinders to cancel all external magnetic fields. The photoelectron energy resolution, obtained under coincidence conditions, is at least 30meV as measured on Ar^+/e^- coincidence data. Photoion kinetic energy distributions are measured by a retarding potential analyser and a half-width half-maximum of 30 meV is measured for the thermal energy distribution of molecular ions, e.g. Ar^+ or CO_2^+. The electron and ion detectors are conventional 17-stage electron multipliers with 20 ns FWHM output pulses. The power supplies used to drive both the ion and electron optics are programmable by an IBM 486DX PC, through a serial RS-232 input-output port.

Perpendicular to the photoion photoelectron optical axis, the light produced by a discharge lamp (Helectros) is introduced into the ion chamber through a capillary 0.5 mm in diameter. A photoelectric light detector is placed opposite and coaxially to monitor continuously the light source.

The whole experiment is contained in a vacuum vessel which is baked out at about 250°C and an ultimate vacuum lower than 10^{-8}Torr is obtained. For the recording of the photoelectron spectra and ion kinetic energy distributions the gas sample is introduced at about 2 x 10^{-5} Torr. For coincidence and time-of-flight (TOF) measurements the sample pressure is reduced to pressures lower than 2xl0^{-6}Torr for better coincidence statistics [10].

The hardware and software for the data acquisition in the TOF, PIPECO, photoion kinetic energy and mass spectrum measuring modes were developed and installed on an FPGA-based (field programmable gate array), home-made interface inserted in the IBM PC. Additional external modules were built for the TOF measurement and the implementation of coincidence gates.

Details of the construction of this instrument and the hardware and electronic circuitries used in this experiment as well as the performance tests made on Ar and O_2 will be reported and discussed in detail in a forthcoming publication [10].

3. EXPERIMENTAL RESULTS AND DISCUSSION

The carbon dioxide sample used in this work, purchased from Air Liquide, is of 99.998% purity and is introduced without further purification. The first ionization energy of the $X^2\Sigma_g^+$ state of CO_2 at 13.7778 ± 0.0001 eV [9] is used for the photoelectron energy scale calibration. The background mass spectrum, recorded with the He(I) resonance line, is shown to be nitrogen and oxygen free. No interference with CO^+ and O^+ from CO_2 is suspected.

The retarding potential energy curves of the fragment ions have been recorded at 21.22 eV. Their first derivative, representing the translational energy distribution, is represented in Fig. 1. Both 0^+ (see Fig. 1(a)) and CO^+ (see Fig. 1 (b)) are displayed together with CO_2^+ for comparison and for the retarding potential energy (V_R) scale calibration.

Up to about 40meV the CO^+ ion energy distribution is almost equal to the purely thermal CO_2^+ distribution. At higher energies and up to 280 meV, energetic CO^+ ions bring a measurable contribution. The production of energetic O^+ at 21.22 eV is more clearly visible (see Fig. 1(a)) and extends to about 390 meV. A contribution from the He(II) resonance line to the high energy side of both these distributions could not be excluded. A weak He^+ ion signal is observed at *m/z* 4. These translational energy distribution results could only be compared with our previous electron impact data [1]. The kinetic energy versus appearance energy diagrams of O^+ and CO^+ show 400 meV ions for both species at 21.2 eV electron energy. However, in both cases the data had to be interpreted by the excess energy partitioning between translational and internal energy of the diatomic CO or CO^+ fragment.

Published in: International Journal of Mass Spectrometry and Ion Processes (1995), vol.. 148, pp. L17-L23.
Status: Postprint (Author's version)

Fig. 1. *First differentiated retarding potential curves of O^+ (a) and CO^+ (b) from CO_2 (dots) measured at 21.22eV photon energy. The CO_2^+ thermal energy distribution (continuous line) is shown for comparison.*

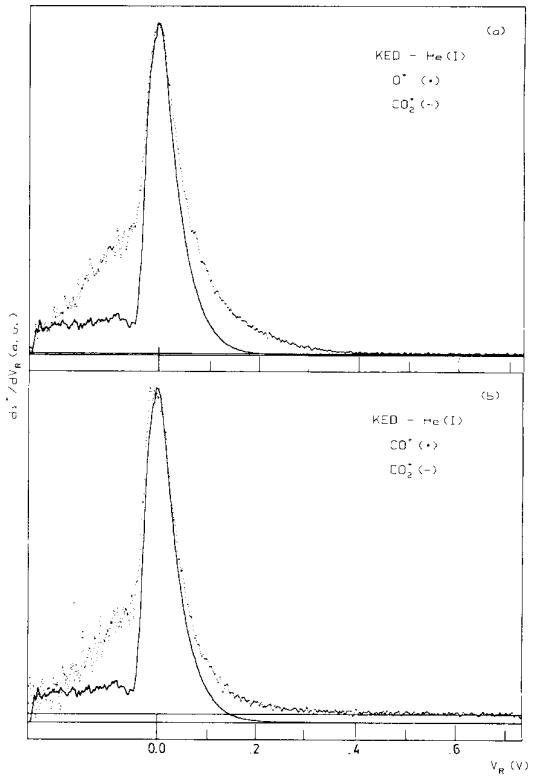

Fig. 2*. Time-of-flight (TOF) distribution of O^+ (a), CO^+ (b) and CO_2^+ (c) observed in coincidence with $CO_2^+(C^2\Sigma_g^+$, υ = 0,0,0) and $CO_2^+(B^2\Sigma_u^+$, υ = 0,0,0) photoelectons. The measured TOF maximum is indicated for each ion.*

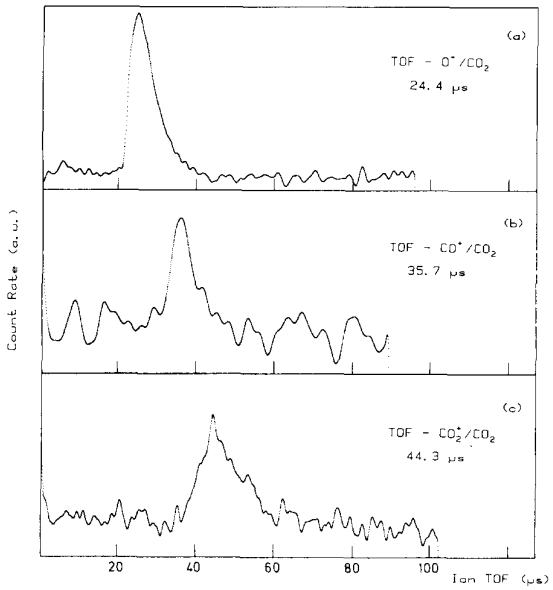

Published in: International Journal of Mass Spectrometry and Ion Processes (1995), vol.. 148, pp. L17-L23.
Status: Postprint (Author's version)

Fig. 3. *Photoelectron and photoion-photoelectron coincidence spectra of CO_2 (a), O^+ (b), CO^+ (c) and CO_2^+ (d) respectively. TOF windows of 10 μs are centred on the maxima indicated in Fig.* 2.

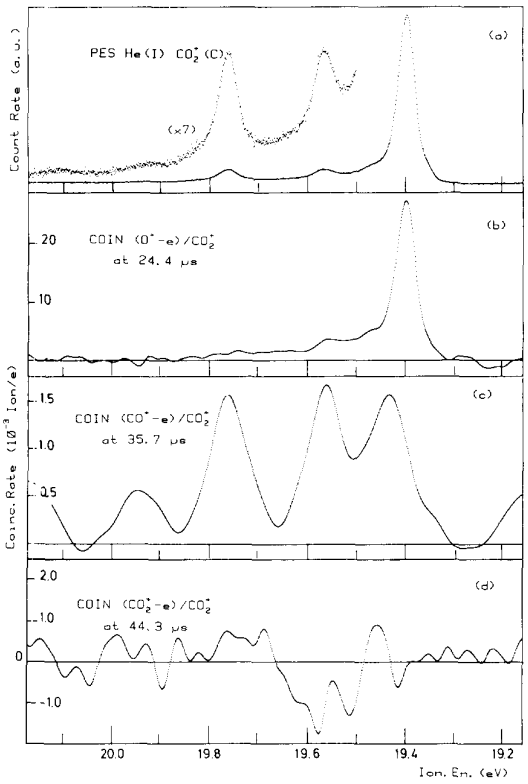

The kinetic energy distribution should be related to the TOF of the ions. The TOFs of the three species observed with He(I) radiation have been recorded and are shown in Fig. 2. The two fragment ions CO^+ and O^+ are measured in coincidence with CO_2^+ ($C^2\Sigma_g^+$, υ = 0,0,0) photoelectrons, whereas the CO_2^+ ions are observed in coincidence with CO_2^+($B^2\Sigma_u^+$, υ = 0,0,0) photoelectrons. The maxima of the TOF distribution corresponding to O^+, CO^+ and CO_2^+ are measured at 24.4μs, 35.7μs and 44.3μs respectively. These are recorded under strictly identical ion optical conditions, e.g. 50meV extraction field. The time resolution of the TOF scaler is 62 ns.

The present TOF results have to be compared with the PIPECO results published by Bombach et al. [7]. For the O^+ ion the shapes of the TOF distributions are very similar, with a steeply rising portion at 20μs, ascribed to energetic ions, and a slowly decreasing portion including thermal O^+ ions. The CO^+ TOF distribution, recorded for CO_2^+($C^2\Sigma_g^+$, υ = 0,0,0) electrons, has a profile fairly similar to that of the parent ion, essentially tailing in the high TOF direction (owing to the low extraction field). It could not be compared with the result of Bombach et al. [7] who measured a TOF of CO^+ for (i) CO_2^+($C^2\Sigma_g^+$, υ = 1,0,1) electrons and (ii) using an extraction field of 2 V cm^{-1}.

The full TOF windows, as displayed in Fig. 2, were used to record the PIPECO spectra of the three ionic species, i.e. O^+, CO^+ and CO_2^+ observed in the 21.22eV mass spectrum of CO_2. The result is shown in Fig. 3.

The photoelectron spectrum of the CO_2^+ ($C^2\Sigma_g^+$) ionic state, as measured under coincidence conditions, has been reproduced between 19.2 and 20.1 eV (see Fig. 3(a)). The entire vibrational structure is observed. Only the Fermi resonance (0,2,0/1,0,0) doublet [9] is not resolved in the present work.

Using a window of l0μs centred on TOF(CO_2^+) = 44.3μs, the coincidence spectrum of CO_2^+ only shows a signal randomly distributed about the base line (see Fig. 3(d)). No signal correlated with the photoelectron spectrum is observed in the 19.2-20.1 eV ionization energy range. This clearly means that the CO_2^+ molecular ions do not survive the dissociation in this energy range. The present observation generalizes the experimental results of Eland [3] and Frey et al. [4] who restricted their observations to the CO_2^+ ($C^2\Sigma_g^+$) adiabatic ionization energy onset region using PIPECO and TPES coincidence measurements respectively.

Published in: International Journal of Mass Spectrometry and Ion Processes (1995), vol.. 148, pp. L17-L23.
Status: Postprint (Author's version)

Table 1 *The vibrational assignment (v_1, v_2, v_3) of the CO_2^+ ($C^2\Sigma_g^+$) state, the corresponding ionization energy (IE) (eV) reported in the literature[9] compared with the results of the present work and the branching ratio b of each vibrational level in the CO^+ and O^+ channels*

	CO_2^+ ($C^2\Sigma_g^+$)		Branching ratio			
(v_1,v_2,v_3)	IE		$b(CO^+)$		$b(O^+)$	
	This work	[9]	This work	Lit.	This work	Lit.
0,0,0	19.394	19.3944	0.05[8]	0.11[b] 0.06[c]	0.94[2]	0.89[b] 0.94[c]
0,1,0	19.449	19.4705	0.31[7]	-	0.68[3]	-
0,2,0	n.r.	19.5432	-	-	-	-
1,0,0	19.557	19.5660	0.42[8]	1.00[c]	0.57[1]	0.00
1,0, 1	19.758	19.7568	1.00	1.00[c]	0.00	0.00
2,0, 1	19.939	19.9268	1.00	-	0.00	-

n.r., not resolved.
[a] Estimated error is ± 0.01.
[b] In Ref. [4] mentioned error ± 0.16.
[c] In Ref. [7] mentioned error ± 0.01.

In contrast, for the CO^+ and O^+ fragment ions a strongly correlated coincidence signal is observed in both dissociation channels as shown in Figs. 3(b) and 3(c). The coincidence rates are given in ion/e^- units and the scaling differences of the ordinate of Figs. 3(b), 3(c) and 3(d) have to be noted. From these data the branching ratio of each vibrational level in the two dissociation channels is measured and is listed in Table 1. Implicitly the ion transmission function of the ion optics and mass spectrometer has been assumed to be constant for *m/z* 16 and 28. The amount of trans-lational energy carried by O^+ and CO^+ being of the same order of magnitude, the discrimination due to this effect is negligible. In the same table the ionization energies and vibrational assignments from the literature [9] and the results of the present work are displayed.

The O^+ coincidence spectrum extends up to 19.55eV. The structures corresponding to the (0,0,0), (0,1,0) and (1,0,0) vibrational levels, respectively, are clearly identified. At higher energies the coincidence spectrum continuously decreases and oscillates about the base line. Unequivocally, the O^+ ion production is limited to these three vibrational levels of the CO_2^+ ($C^2\Sigma_g^+$) state. Bombach et al. [7] considered the O production to be restricted to the $C^2{}_g^+$ (0,0,0) level only and to be completely quenched at higher ionization energies. This is iΣn disagreement with the present work. On the basis of the measured intensities, 75.5%, 14.5% and 9.8% of the total O^+ ions originate from the (0,0,0), (0,1,0) and (1,0,0) levels respectively.

Energetically, in the CO_2^+ ($C^2\Sigma_g^+$) state the dissociative ionization reaction

$$CO_2 + h\nu \rightarrow CO_2^+(C^2\Sigma_g^+, v_1, v_2, v_3) + e^-$$
$$\xrightarrow[^4\Sigma^+]{\text{pred.}} O^+(^4S_u) + CO(X^1\Sigma^+, v)$$

is accessible where the neutral CO fragment could be produced in the vibrational ground and first excited states. The production of CO($X^1\Sigma^+$, *v=2)* would need 19.597eV [1,12] and is therefore not allowed, no significant contribution of O^+ being detected above 19.566eV. This process has been extensively discussed earlier [1,7], and Bombach et al. [7], Eland [6] and Frey et al. [4] were able to measure the branching ratio for the unimolecular decomposition of the $C^2\Sigma_g^+$ (0,0,0) level into CO($X^1\Sigma^+$, υ = *0)* and CO($X^1\Sigma^+$, υ = 1) levels, i.e. 0.56 ± 0.1 [7] or 0.12-0.33 [4,6] and 0.38 ± 0.1 [7] or 0.67-0.88 [4,6] respectively. These latter measurements were based upon TOF distribution fittings. This data handling is difficult in the present experiment owing to the weakness of the extraction field used to preserve a good electron energy resolution, but at the expense of the time resolution.

Fig. 3(c) shows that the CO^+ coincidence spectrum is spread over the whole ionization energy range studied. This spectrum strongly correlates with the CO_2^+ ($C^2\Sigma_g^+$) photoelectron spectrum displayed in Fig. 3(a). Only part of the (0,0,0) level gives rise to CO^+ at a rate *b* = 5.8% (see Table 1), as measured at an energy of 19.39eV, corresponding to the adiabatic ionization energy. The maximum of the first peak corresponds to the (0,1,0) vibrational level. Besides this peak, the (0,2,0), (1,0,0), (1,0,1) and the (2,0,1) levels are unequivocally

present in the coincidence spectrum. The branching ratio for CO^+ production (see Table 1) regularly increases and up from the (1,0,1) level, O^+ ion formation being entirely quenched, only the CO^+ ions are formed.

$$CO_2 + h\nu \rightarrow CO_2^+(C^2\Sigma_g^+, v = 0,0,0, J^*) + e^-$$

$$\xrightarrow[^2\Pi_u]{\text{pred.}} CO^+(X^2\Sigma^+, v = 0) + O(^3P_g)$$

The energetics of CO^+ ion production from CO_2 shows that the ions originate from the reaction for which the threshold is calculated at 19.465eV [1], i.e. above the energy level of the $C^2\Sigma_g^+$ (0,0,0) state. This fragmentation has to involve high rotationally excited CO_2^+ ($C^2\Sigma_g^+$, v — 0,0,0) ions. This process has been extensively discussed earlier by Bombach et al. [7]. The branching ratio is about 6% (see Table 1) in the CO^+ channel, in agreement with previous reports [6,7]. This picture is only valid for the $CO_2^+(C^2\Sigma_g^+, \upsilon = 0,0,0)$ state and when the branching ratio is measured at 19.39 eV.

The present measurements unequivocally show that the branching ratio for CO^+ production is far from unity [7] at higher energy (see Table 1). The competition between unimolecular decomposition into $CO^+ + O$ and $O^+ + CO$ is still observed at higher energies. Contrary to previous results the *b* value slowly increases and only becomes unity above 19.758 eV. At this level enough energy is available for producing vibrationally excited CO^+ ($X^2\Sigma^+$) species. This would corroborate our previous electron impact results [1] where the slope of the kinetic energy versus appearance energy diagram could be accounted for by the reaction

$$CO_2^+ \rightarrow O^+(^3P_g) + CO(X^2\textstyle\sum^+, \upsilon = 1)$$

below 19.94eV and corresponding to the upper energy limit of the Franck-Condon transitions induced by the He(I) resonance line. Above 19.94eV, dissociative autoioniza-tion has been invoked [1]. This could only be checked by threshold photoelectron-photoion coincidence spectroscopy.

4. CONCLUSIONS

The main goal of this Letter was to report recent results on the dissociative photoioniza-tion of CO_2 obtained with a newly built photo-ion-photoelectron spectrometer. This work was undertaken to add more details to our recent dissociative electroionization work on this molecule. Though PIPECO results were already available, owing to the particular working conditions maintained in the present experiment, we were able to measure coincidences under high resolution conditions, resolving practically the entire vibrational structure of the CO_2^+ ($C^2\Sigma_g^+$) state. The O^+ ions are shown to be produced up to 19.57 eV whereas the CO^+ fragment is observed up to 19.94 eV. The branching ratios for both species at all vibrational levels of CO_2^+ ($C^2\Sigma_g^+$) are measured.

ACKNOWLEDGEMENTS

The Université de Liège, the Fonds National de la Recherche Scientifique (FNRS) and the Fonds de la Recherche Fondamentale Collective (FRFC contract no 2.4537.91 and 2.4532.95) are acknowledged for financial support. Professor Paul Natalis is gratefully acknowledged for his critical reading of the manuscript.

REFERENCES

[1] R. Locht and M. Davister, Int. J. Mass Spectrom. Ion Processes, 144(1995) 105.

[2] K.E. McCulloh, J. Chem. Phys., 59 (1973) 4250.

[3] J.H.D. Eland and J. Berkowitz, J. Chem. Phys., 67 (1977) 2782.

[4] R. Frey, B. Gotchev, O.F. Kalman, W.B. Peatman, H. Pollak and E.W. Schlag, Chem. Phys., 21 (1977) 89.

[5] T. Baer and P.M. Guyon, J. Chem. Phys., 85 (1986) 4765.

[6] J.H.D. Eland, Int. J. Mass Spectrom. Ion Phys., 9 (1972) 397.

[7] R. Bombach, J. Danacher, J.P. Stadelmann and J.C. Lorquet, J. Chem. Phys., 79 (1983) 4214.

[8] R. Locht, M. Davister, W. Denzer, H.W. Jochims and H. Baumgärtel, Chem. Phys., 138 (1989) 433.

[9] L.S. Wang, J.E. Reutt, Y.T. Lee and D.A. Shirley, J. Electron Spectrosc. Relat. Phenom., 47 (1988) 167.

[10] Ch. Servais and R. Locht, Int. J. Mass Spectrom. Ion Processes, submitted for publication.

[11] I. Lindau, J.C. Helmer and J. Uebbing, Rev. Sci. Instrum., 44(1973)265.

[12] P.H. Krupenie, The Band Spectrum of Carbon Monoxide, NSRDS-NBS 5 (1966), US Print Office, Washington, DC, 20234.